YMTHE, Volume *30*

Supplemental Information

Identification of FDA-approved bifonazole as a SARS-CoV-2 blocking agent following a bioreporter drug screen

Zaid Taha, Rozanne Arulanandam, Glib Maznyi, Elena Godbout, Madalina E. Carter-Timofte, Naziia Kurmasheva, Line S. Reinert, Andrew Chen, Mathieu J.F. Crupi, Stephen Boulton, Geneviève Laroche, Alexandra Phan, Reza Rezaei, Nouf Alluqmani, Anna Jirovec, Alexandra Acal, Emily E.F. Brown, Ragunath Singaravelu, Julia Petryk, Manja Idorn, Kyle G. Potts, Hayley Todesco, Cini John, Douglas J. Mahoney, Carolina S. Ilkow, Patrick Giguère, Tommy Alain, Marceline Côté, Søren R. Paludan, David Olagnier, John C. Bell, Taha Azad, and Jean-Simon Diallo

SUPPLEMENTARY INFORMATION

Supplementary Figures

A)

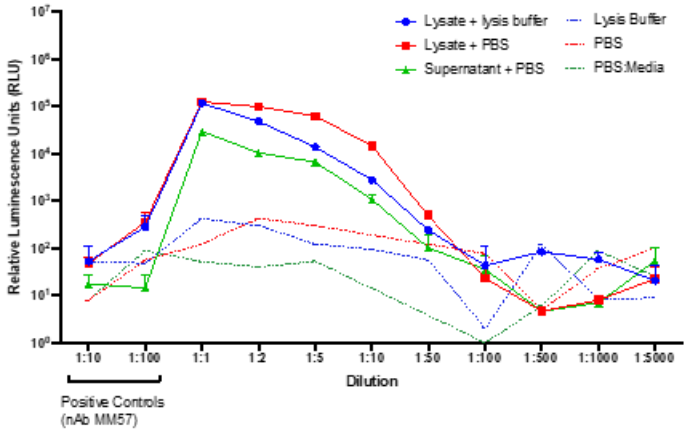

B)

Protocol	*Dynamic Range (RLU)*	*Z-factor*
Method A	*936.460*	*0.915*
Method B	*1834.636*	*0.687*

C)

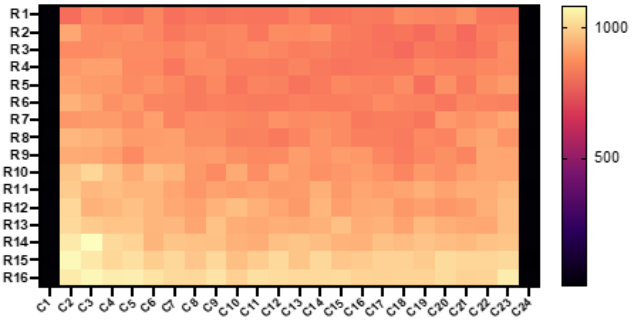

Mean	*867.08*
STDev	*75.53*
%CV	*8.71*

D)

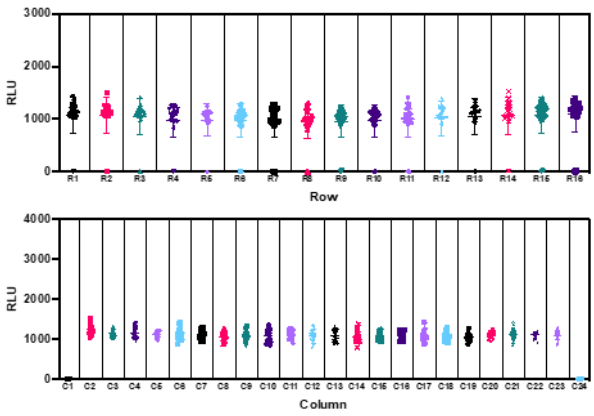

E)

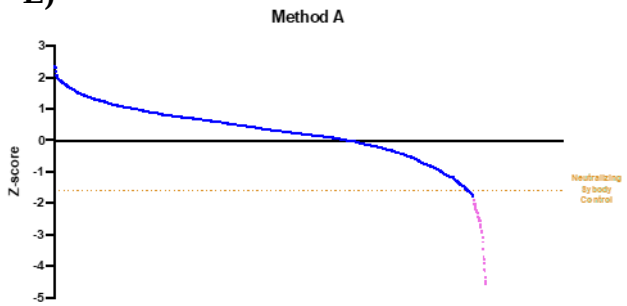

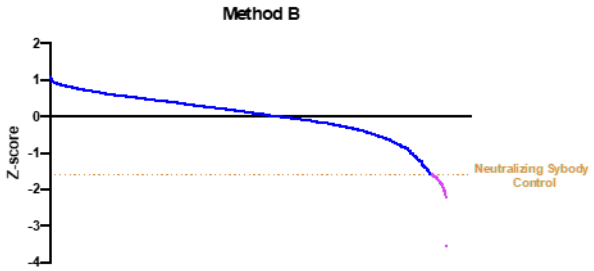

F)

Method A	Normalized to DMSO (per row)				
	Sorted by fold-change				
Sample ID	**Fold change**	**p-value**	**-log(p-value)**	**q-value**	**-log(q-value)**
Prestw-299	-0.500	1.85E-01	7.32E-01	2.98E-04	3.53E+00
Prestw-300	-0.484	3.57E-02	1.45E+00	6.77E-05	4.17E+00
Prestw-1241	-0.456	9.34E-01	2.97E-02	3.13E-03	2.51E+00
Prestw-1341	-0.424	6.05E-01	2.18E-01	1.13E-03	2.95E+00
Prestw-383	-0.379	7.40E-01	1.31E-01	1.60E-03	2.80E+00
Prestw-304	-0.358	9.72E-01	1.22E-02	4.12E-03	2.38E+00
Prestw-1407	-0.336	9.73E-01	1.19E-02	4.15E-03	2.38E+00
Prestw-789	-0.305	1.49E-01	8.27E-01	2.47E-04	3.61E+00
Prestw-1051	-0.301	6.48E-01	1.89E-01	1.26E-03	2.90E+00
Prestw-389	-0.293	9.27E-01	3.27E-02	3.03E-03	2.52E+00
Prestw-1405	-0.265	7.43E-01	1.29E-01	1.61E-03	2.79E+00
Prestw-260	-0.256	5.70E-02	1.24E+00	1.01E-04	3.99E+00
Prestw-1452	-0.235	9.97E-01	1.40E-03	6.63E-03	2.18E+00
Prestw-1358	-0.218	1.00E+00	5.94E-06	1.35E-02	1.87E+00
Prestw-267	-0.211	1.00E+00	2.00E-06	1.50E-02	1.82E+00
Prestw-1019	-0.209	1.00E+00	8.47E-05	1.01E-02	2.00E+00
Prestw-1105	-0.183	7.98E-01	9.81E-02	1.87E-03	2.73E+00
Prestw-752	-0.183	1.63E-01	7.88E-01	2.64E-04	3.58E+00
Prestw-295	-0.174	1.00E+00	3.18E-07	1.75E-02	1.76E+00
Prestw-430	-0.163	1.00E+00	9.16E-11	2.97E-02	1.53E+00
Prestw-525	-0.156	6.25E-01	2.04E-01	1.18E-03	2.93E+00
Prestw-1197	-0.153	1.00E+00	2.95E-06	1.44E-02	1.84E+00
Prestw-1236	-0.149	1.57E-04	3.80E+00	9.38E-07	6.03E+00
Prestw-793	-0.146	8.07E-01	9.30E-02	1.93E-03	2.72E+00
Prestw-227	-0.145	1.00E+00	6.83E-06	1.33E-02	1.88E+00
Prestw-58	-0.142	9.99E-01	2.64E-04	8.66E-03	2.06E+00

Method B	Normalized to DMSO (per row)				
	Sorted by difference				
Sample ID	**Fold change**	**p-value**	**-log(p-value)**	**q-value**	**-log(q-value)**
Prestw-1241	-0.512	1.56E-05	4.81E+00	5.69E-06	5.24E+00
Prestw-299	-0.252	4.01E-06	5.40E+00	2.07E-06	5.68E+00
Prestw-304	-0.231	4.99E-06	5.30E+00	2.42E-06	5.62E+00
Prestw-1407	-0.178	1.11E-05	4.95E+00	4.37E-06	5.36E+00
Prestw-383	-0.168	1.48E-08	7.83E+00	3.34E-08	7.48E+00
Prestw-260	-0.158	7.66E-06	5.12E+00	3.28E-06	5.48E+00
Prestw-1051	-0.151	4.22E-04	3.37E+00	8.60E-05	4.07E+00
Prestw-430	-0.139	4.16E-04	3.38E+00	8.51E-05	4.07E+00
Prestw-1341	-0.136	6.87E-04	3.16E+00	1.30E-04	3.89E+00
Prestw-300	-0.134	2.17E-06	5.66E+00	1.32E-06	5.88E+00
Prestw-1405	-0.134	8.06E-03	2.09E+00	1.22E-03	2.92E+00
Prestw-1	-0.133	2.79E-02	1.55E+00	3.93E-03	2.41E+00
Prestw-1105	-0.133	7.64E-04	3.12E+00	1.43E-04	3.84E+00
Prestw-520	-0.129	4.24E-07	6.37E+00	3.81E-07	6.42E+00
Prestw-1310	-0.114	1.51E-03	2.82E+00	2.58E-04	3.59E+00
Prestw-1019	-0.091	1.01E-03	2.99E+00	1.81E-04	3.74E+00
Prestw-81	-0.087	4.68E-02	1.33E+00	6.43E-03	2.19E+00
Prestw-1021	-0.084	7.59E-03	2.12E+00	1.15E-03	2.94E+00
Prestw-525	-0.083	1.02E-01	9.90E-01	1.36E-02	1.87E+00
Prestw-752	-0.075	1.09E-03	2.96E+00	1.94E-04	3.71E+00
Prestw-1157	-0.071	1.59E-02	1.80E+00	2.30E-03	2.64E+00
Prestw-1423	-0.070	1.48E-07	6.83E+00	1.63E-07	6.79E+00
Prestw-438	-0.069	3.88E-04	3.41E+00	8.06E-05	4.09E+00
Prestw-789	-0.064	2.88E-03	2.54E+00	4.65E-04	3.33E+00
Prestw-2	-0.060	1.27E-01	8.96E-01	1.68E-02	1.78E+00
Prestw-1409	-0.057	1.71E-05	4.77E+00	6.12E-06	5.21E+00
Prestw-641	-0.056	2.54E-02	1.59E+00	3.60E-03	2.44E+00
Prestw-1449	-0.056	5.26E-02	1.28E+00	7.19E-03	2.14E+00
Prestw-1152	-0.056	1.65E-03	2.78E+00	2.80E-04	3.55E+00
Prestw-487	-0.049	2.36E-08	7.63E+00	4.35E-08	7.36E+00
Prestw-1270	-0.048	2.74E-02	1.56E+00	3.86E-03	2.41E+00
Prestw-1125	-0.043	4.34E-02	1.36E+00	5.99E-03	2.22E+00
Prestw-970	-0.042	1.39E-04	3.86E+00	3.40E-05	4.47E+00
Prestw-1110	-0.040	1.12E-07	6.95E+00	1.36E-07	6.87E+00
Prestw-1049	-0.035	1.16E-06	5.94E+00	8.21E-07	6.09E+00

Supplementary Figure 1. Nanoluciferase complementation bioreporter screen identifies subset of FDA-approved compound library as potential SARS-CoV-2 blocking agents. (A-D) Optimization and validation of biosensor high throughput screen format parameters. (A) Titration of bioreporter harvested from whole cell lysates or cell supernatants. The bioreporter was diluted using lysis buffer, PBS, or DMEM (PBS Media) and signal was read by addition of CTZ substrate. (B) Assessment of statistical effect size and signal-to-noise by determination of dynamic range and Z-factor for both Method A and Method B. (C) Determination of high throughput signal variability; 24 ul of LgBiT-RBD and 24 ul of ACE2-SmBiT were dispensed into a 384-well plate and incubated at 37C for 30 minutes. Luminescence signal was read following addition of CTZ substrate. (D) Luminescence signal intensity of each well from (C) was plotted to identify column or row effects. **E)** Z-scores from both Method A and Method B were calculated and graphed. The neutralizing Sybody control from Method B is indicated by the orange horizontal line as a reference point for signal inhibition. Points plotted in magenta represent compounds that impair bioreporter luminescence to levels equal to or lower than the Sybody control. **F)** Shortlisted candidate compounds from both Method A and Method B listed in order of decreasing fold-change in signal intensity.

A)

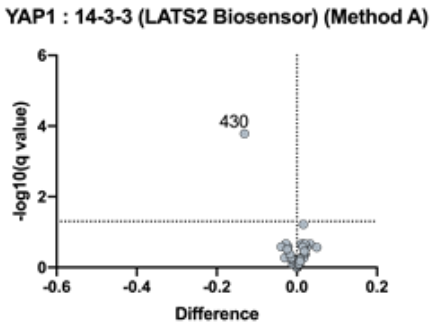

B)

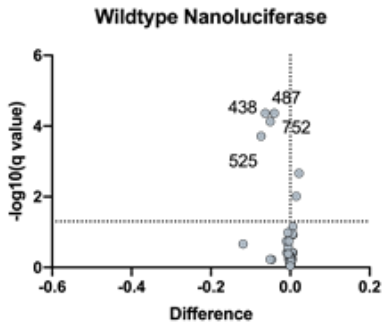

C)

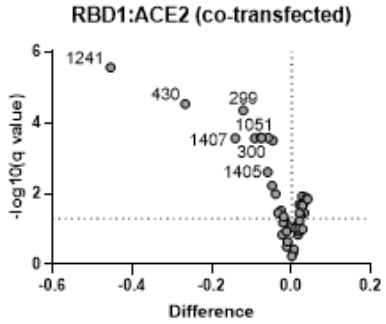

D)

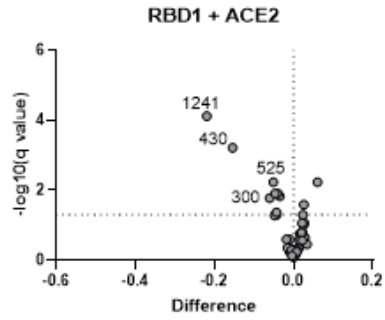

E)

		SARS-CoV2-RBD		SARS-CoV2-S1		SARS-CoV-RBD	
	Compound	ACE2+RBD2	RBD2 : ACE2	ACE2+Spike	Spike : ACE2	ACE2+RBD1	RBD1 : ACE2
Prestw-1241	Bifonazole	-0.23	-0.22	-0.29	-0.05	-0.45	-0.22
Prestw-1405	Ethinylestradiol	-0.05	-0.04	-0.06	n.s.	-0.06	-0.04
Prestw-383	Nicardipine hydrochloride	-0.05	n.s.	n.s.	-0.05	-0.05	-0.03
Prestw-430	Cisapride	-0.19	-0.08	-0.07	-0.06	-0.27	-0.15

F)

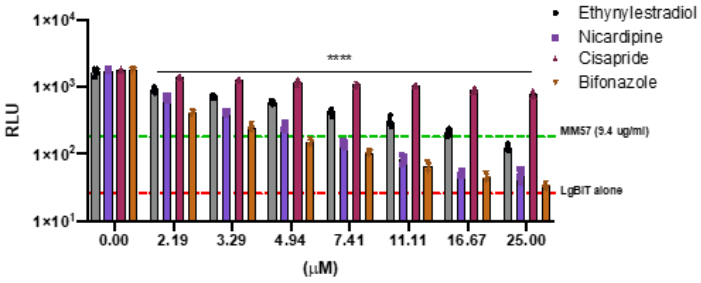

G)

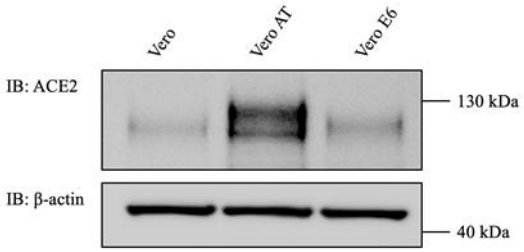

H)

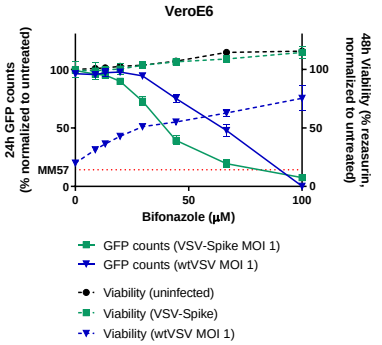
VeroE6
24h GFP counts (% normalized to untreated)
48h Viability (% rezasurin, normalized to untreated)
MM57
Bifonazole (μM)
GFP counts (VSV-Spike MOI 1)
GFP counts (wtVSV MOI 1)
Viability (uninfected)
Viability (VSV-Spike)
Viability (wtVSV MOI 1)

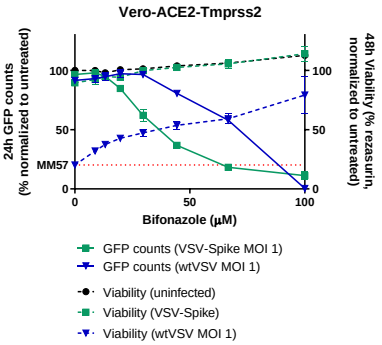
Vero-ACE2-Tmprss2
24h GFP counts (% normalized to untreated)
48h Viability (% rezasurin, normalized to untreated)
MM57
Bifonazole (μM)
GFP counts (VSV-Spike MOI 1)
GFP counts (wtVSV MOI 1)
Viability (uninfected)
Viability (VSV-Spike)
Viability (wtVSV MOI 1)

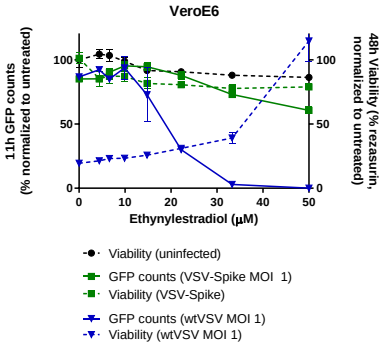
VeroE6
11h GFP counts (% normalized to untreated)
48h Viability (% rezasurin, normalized to untreated)
Ethynylestradiol (μM)
Viability (uninfected)
GFP counts (VSV-Spike MOI 1)
Viability (VSV-Spike)
GFP counts (wtVSV MOI 1)
Viability (wtVSV MOI 1)

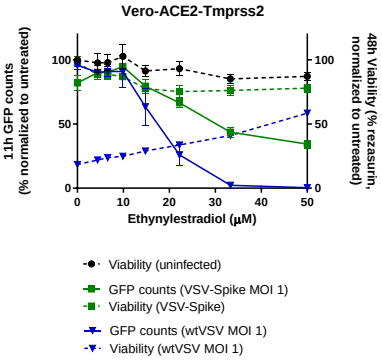
Vero-ACE2-Tmprss2
11h GFP counts (% normalized to untreated)
48h Viability (% rezasurin, normalized to untreated)
Ethynylestradiol (μM)
Viability (uninfected)
GFP counts (VSV-Spike MOI 1)
Viability (VSV-Spike)
GFP counts (wtVSV MOI 1)
Viability (wtVSV MOI 1)

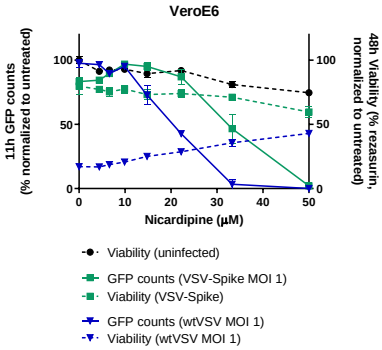
VeroE6
11h GFP counts (% normalized to untreated)
48h Viability (% rezasurin, normalized to untreated)
Nicardipine (μM)
Viability (uninfected)
GFP counts (VSV-Spike MOI 1)
Viability (VSV-Spike)
GFP counts (wtVSV MOI 1)
Viability (wtVSV MOI 1)

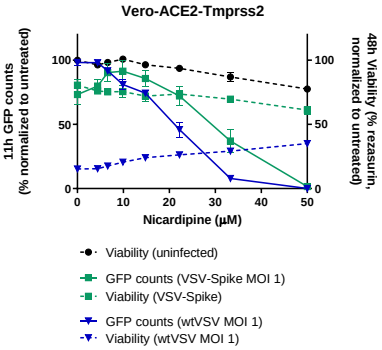
Vero-ACE2-Tmprss2
11h GFP counts (% normalized to untreated)
48h Viability (% rezasurin, normalized to untreated)
Nicardipine (μM)
Viability (uninfected)
GFP counts (VSV-Spike MOI 1)
Viability (VSV-Spike)
GFP counts (wtVSV MOI 1)
Viability (wtVSV MOI 1)

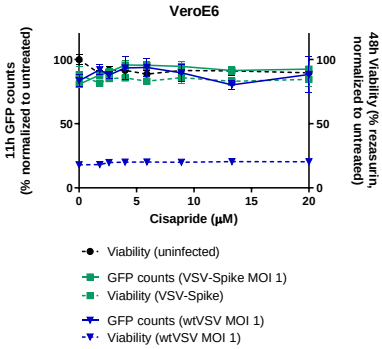
VeroE6
11h GFP counts (% normalized to untreated)
48h Viability (% rezasurin, normalized to untreated)
Cisapride (μM)
Viability (uninfected)
GFP counts (VSV-Spike MOI 1)
Viability (VSV-Spike)
GFP counts (wtVSV MOI 1)
Viability (wtVSV MOI 1)

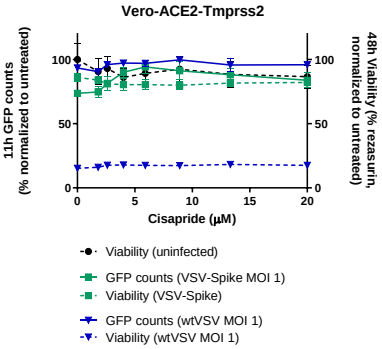
Vero-ACE2-Tmprss2
11h GFP counts (% normalized to untreated)
48h Viability (% rezasurin, normalized to untreated)
Cisapride (μM)
Viability (uninfected)
GFP counts (VSV-Spike MOI 1)
Viability (VSV-Spike)
GFP counts (wtVSV MOI 1)
Viability (wtVSV MOI 1)

I)

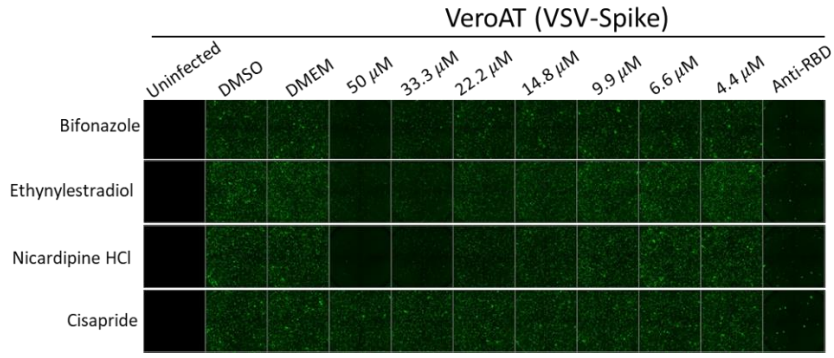

J)

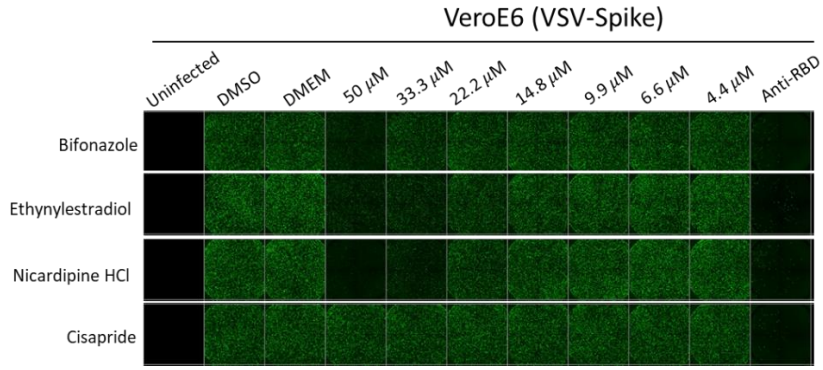

Supplementary Figure 2. Screen validation identifies Bifonazole as top SARS-CoV-2 blocking candidate. A-D) The top 45 hits from our bioreporter screen were added at 4μM final to lysates from cells co-transfected with constructs encoding the non-specific LATS2 biosensor **(A)** wild-type nanoluciferase for non-specific compounds impacting the enzymatic activity of the bioreporter **(B)**, the RBD of SARS-CoV (2002) and ACE2 (method A, **C)** or the RBD of SARS-CoV **(D)** for 50 minutes followed by addition of equal volume of ACE2 and luminescence measured (method B). **E)** Table summarizing fold-change in luminescence signal relative to untreated, obtained from bioreporter validation studies (untreated control = 1.00). **F)** Raw luminescence signal values for bioreporter from Figure 2D. **G)** Whole cell lysates from Vero76, VeroAT, and VeroE6 resolved by PAGE and probed for ACE2 levels and beta-actin as loading control. **H)** Complete dose-response curves of the top 4 compounds displaying % GFP counts and cell viability in VSV-Spike infected, wtVSV infected, and uninfected cells for Figure 2E. **I-J)** Raw fluorescent image montages (2.5X) showing the impact of the top 4 compounds on pseudotyped VSV-Spike-driven GFP expression, in both VeroAT and VeroE6 cells for Figure 2E.

A)

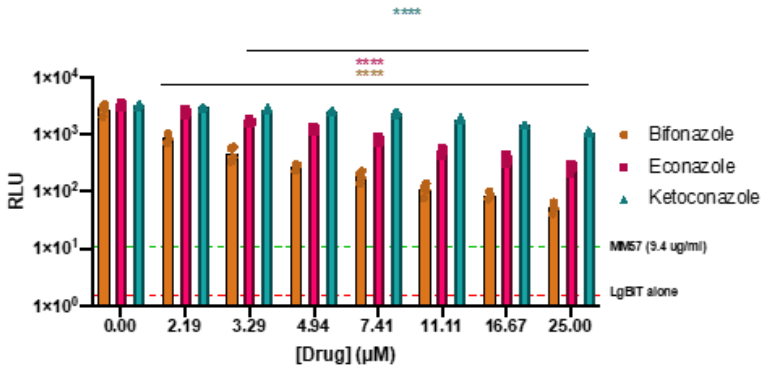
****
****
****
RLU
1×10^4
1×10^3
1×10^2
1×10^1
1×10^0
0.00
2.19
3.29
4.94
7.41
11.11
16.67
25.00
[Drug] (µM)
Bifonazole
Econazole
Ketoconazole
MM57 (9.4 ug/ml)
LgBiT alone

B)

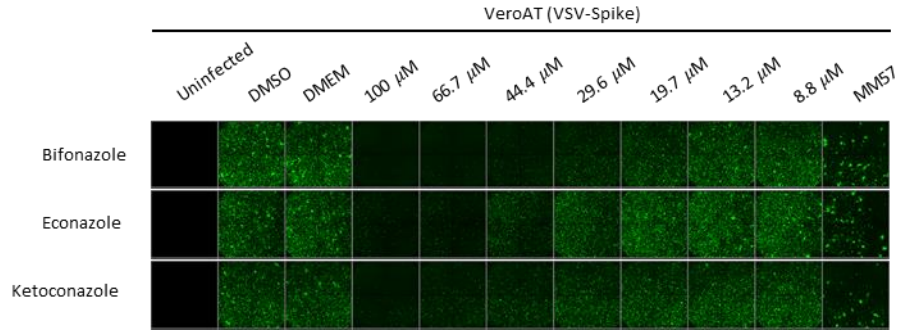
VeroAT (VSV-Spike)
Uninfected
DMSO
DMEM
100 µM
66.7 µM
44.4 µM
29.6 µM
19.7 µM
13.2 µM
8.8 µM
MM57
Bifonazole
Econazole
Ketoconazole

C)

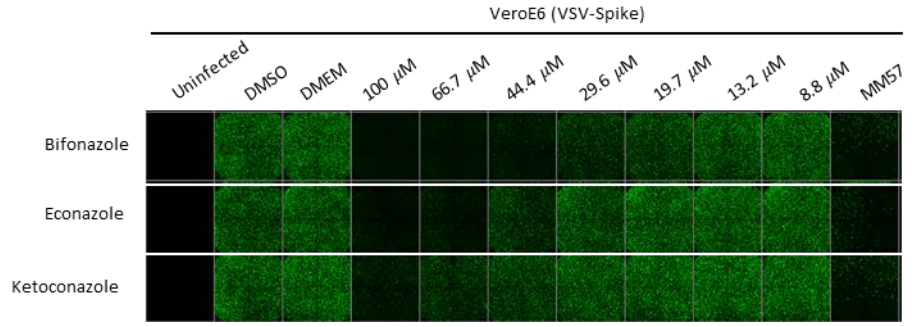
VeroE6 (VSV-Spike)
Uninfected
DMSO
DMEM
100 µM
66.7 µM
44.4 µM
29.6 µM
19.7 µM
13.2 µM
8.8 µM
MM57
Bifonazole
Econazole
Ketoconazole

D)

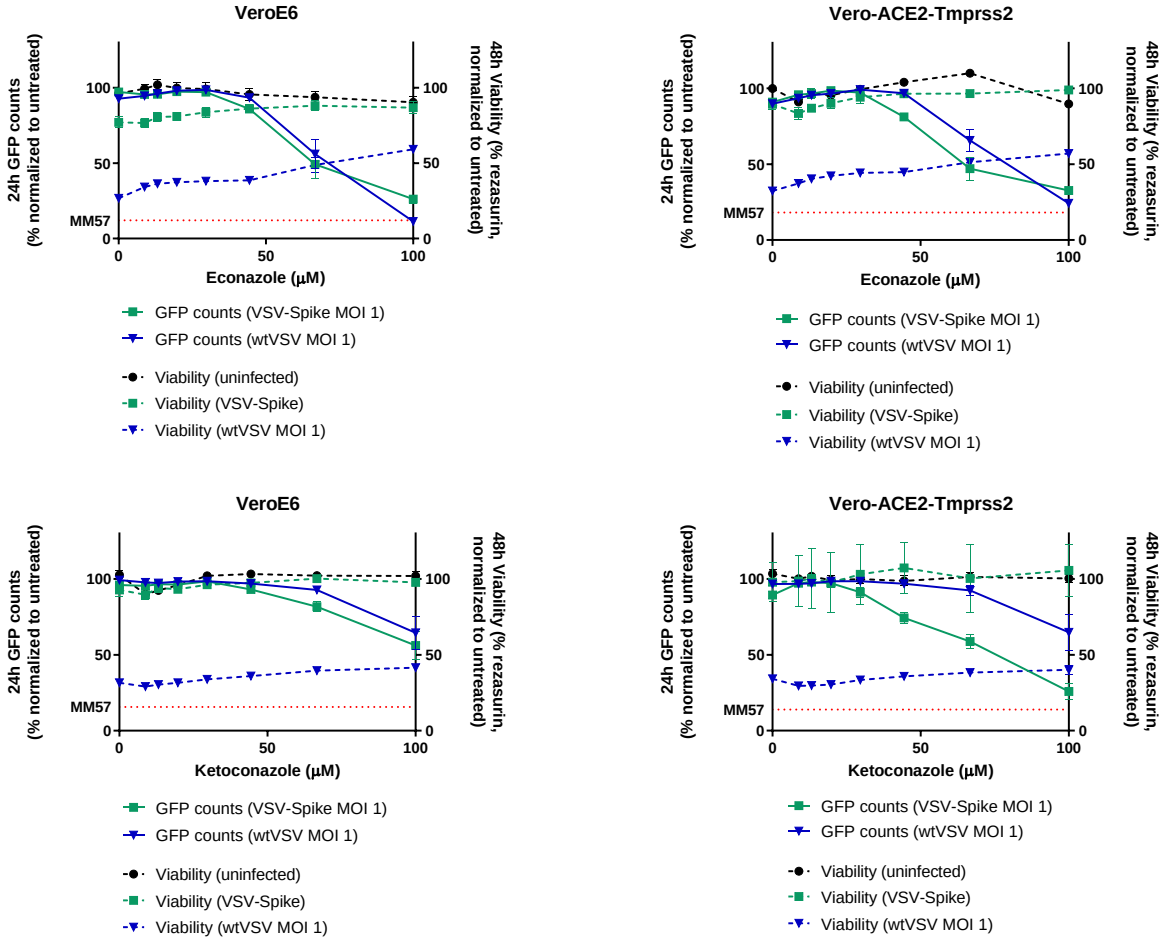

Supplementary Figure 3. Bifonazole outperforms other imidazole antifungals at impairing the interaction between ACE2 and SARS-CoV-2 RBD. (A) Raw luminescence signal values for bioreporter from Figure 3B; dose response of Bifonazole, econazole, and ketoconazole. Average luminescence signal following treatment with anti-RBD neutralizing antibody (MM57) is indicated by the horizontal dotted cyan line. Average luminescence values of the LgBiT-RBD construct alone indicated by the horizontal dotted magenta line **(B-C)** Raw fluorescent image montages (2.5X) showing the impact of the top 3 imidazole antifungal compounds on pseudotyped VSV-Spike-driven GFP expression for Figure 3C. **(D)** Complete dose-response curves of the top 3 imidazole antifungals displaying % GFP counts and cell viability in VSV-Spike infected, wtVSV infected, and uninfected cells for Figure 3C.

A)

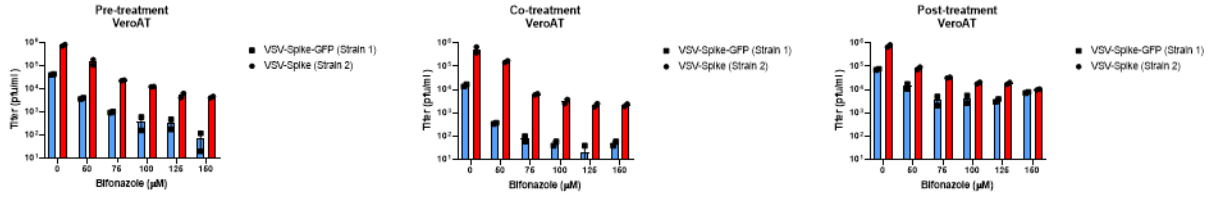
Pre-treatment
VeroAT
Co-treatment
VeroAT
Post-treatment
VeroAT
VSV-Spike-GFP (Strain 1)
VSV-Spike (Strain 2)
Titer (pfu/ml)
Bifonazole (μM)

B)

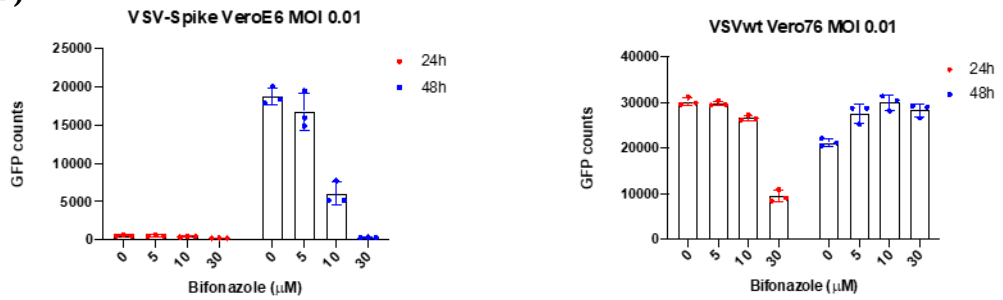
VSV-Spike VeroE6 MOI 0.01
VSVwt Vero76 MOI 0.01
24h
48h
GFP counts
Bifonazole (μM)

C)

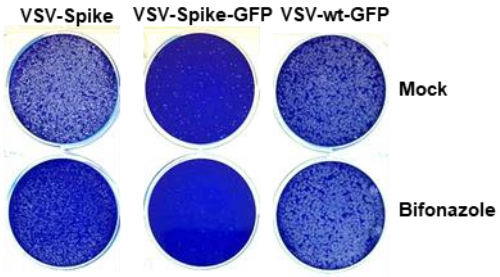
VSV-Spike
VSV-Spike-GFP
VSV-wt-GFP
Mock
Bifonazole

D)

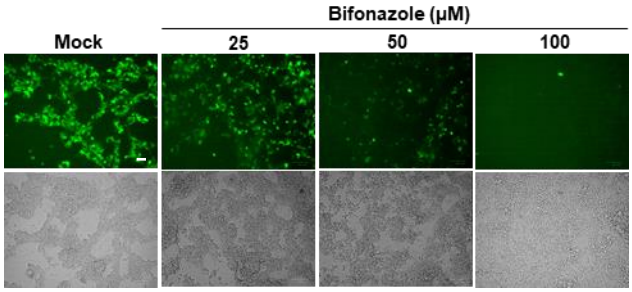
Bifonazole (μM)
Mock
25
50
100

E)

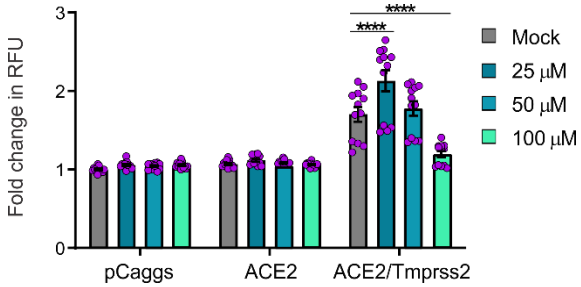
Fold change in RFU
Mock
25 μM
50 μM
100 μM
pCaggs
ACE2
ACE2/Tmprss2
****

F)

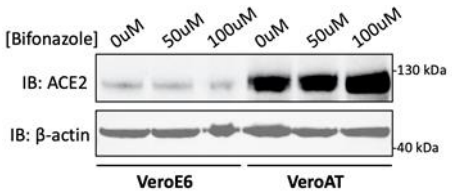
[Bifonazole]
0uM
50uM
100uM
IB: ACE2
IB: β-actin
130 kDa
40 kDa
VeroE6
VeroAT

G)

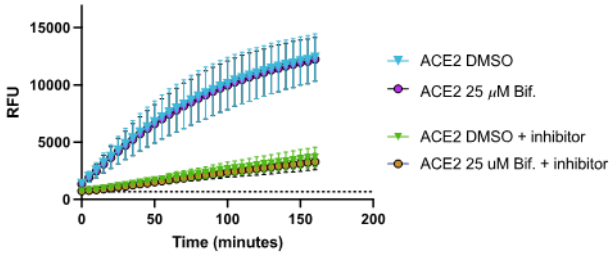
RFU
Time (minutes)
ACE2 DMSO
ACE2 25 μM Bif.
ACE2 DMSO + inhibitor
ACE2 25 uM Bif. + inhibitor

H)

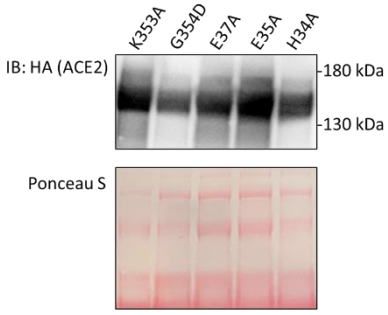
K353A
G354D
E37A
E35A
H34A
IB: HA (ACE2)
180 kDa
130 kDa
Ponceau S

Supplementary Figure 4. Bifonazole impairs viral entry and spread, and interacts with ACE2 to block the RBD binding site of SARS-CoV-2. A) Viral titers measured by standard plaque assay from Figure 4A. **B)** GFP counts from VeroE6 cells treated with Bifonazole and infected with VSV-Spike at MOI 0.01 (left) or Vero76 cells treated with Bifonazole and infected with wtVSV at MOI 0.01 (right). Cells were incubated up to 48 hours post-infection with no replacement of the media and imaged at 24 and 48 hpi. **C)** Plaque expansion assay demonstrating impaired viral spread (i.e. fewer and smaller plaques) of VSV-Spike following treatment of VeroAT cells with 100 μM Bifonazole prior to infection, with no impact on plaque size or count of wtVSV. **D)** HEK293T cells expressing hACE2 or hACE2/TMPRSS2 and Zip-Venus-1 proteins were seeded in 384-well plates and then treated with 0, 25, 50, 100 μM Bifonazole for 30 minutes after which HEK293T cells expressing SARS-CoV-2 Spike and Zip-Venus-2 were added to the wells. Cells were imaged following 3 hours for fusion morphology and Venus fluorescence signal (FITC filter) as a result of zip dimerization yielding to Venus bimolecular fluorescence complementation. (Bottom) Phase contrast and (Top) Venus, bar = 100 μm. **E)** HEK293T cells expressing hACE2 or hACE2/TMPRSS2 and Zip-Venus-1 proteins were seeded in 384-well plates and then treated with 25, 50 or 100 μM Bifonazole for 30 minutes after which HEK293T cells expressing SARS-CoV-1 Spike and Zip-Venus-2 were added to the wells. Cells were imaged after 3 hours for fusion morphology and Venus signal as a result of Venus complementation. Data shows fold change in RFU from 3 independent experiments (n = 12, mean ± SEM; 2-way ANOVA with Dunnett's multiple comparison test over mock-treated for each condition). **F)** VeroE6 or VeroAT cells were treated with Bifonazole at 0, 50, or 100 μM overnight. Whole cell lysates were extracted and resolved by PAGE and probed for ACE2. **G)** Recombinant ACE2 was treated with DMSO or 25 μM Bifonazole, in the presence or absence of an ACE inhibitor. Bifonazole does not impact ACE2 enzymatic activity, and does not interfere with the ACE inhibitor. **H)** 15μl of ACE2 mutant supernatants used in Figure 4H were subject to western blotting for ACE2 (top) and Ponceau stained for total protein detection (bottom).

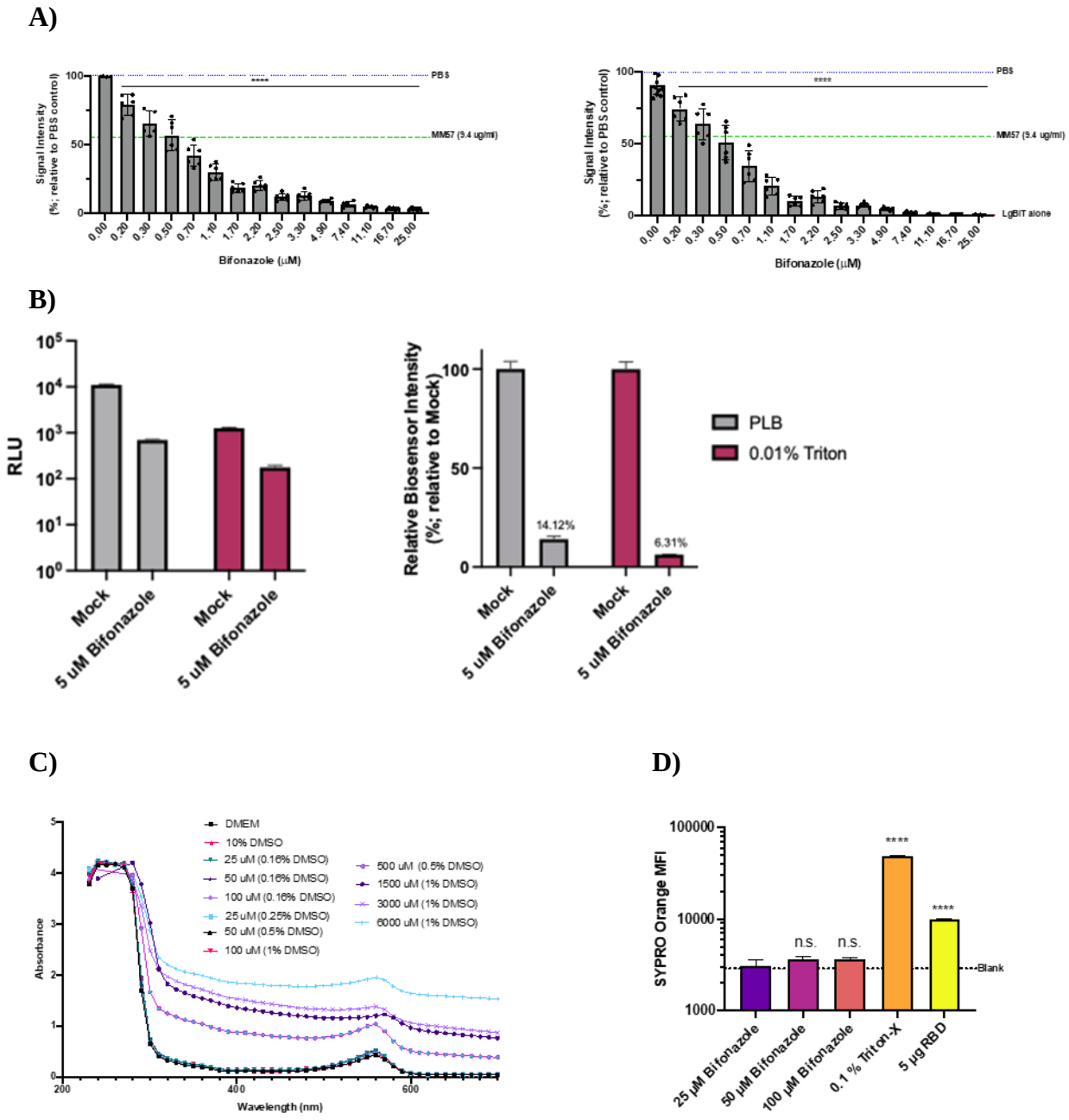

Supplementary Figure 5. Bifonazole does not exert SARS-CoV-2 blocking activity through non-specific interactions of aggregates. A) ACE2 and RBD bioreporters were generated using 10% FBS serum supernatant (left) or serum free supernatant (right). Dose responses are identical in both, suggesting the impact of Bifonazole is not due to solubilizing capacity of serum proteins (n=6, mean ±SEM; one-way ANOVA with Dunnet's test for multiple comparison; values compared against 0 μM control). **B)** ACE2 and RBD bioreporters were prepared from whole cell

lysates harvested using a passive lysis buffer (PLB) or 0.01% Triton-X100 lysis buffer, treated with 5 μM Bifonazole, and luminescence read. Inhibition of luminescence by Bifonazole in both conditions suggests that Bifonazole does not act non-specifically through the formation of micelles, as 0.01% Triton-X100 would disrupt micelle formation. **C)** Spectral analysis of Bifonazole solutions reveals no shifts or aggregate formations in solutions at biologically relevant concentrations (25-100μM in 0.16-1% DMSO). **D)** Bifonazole solutions at biologically relevant concentrations 25-100 μM were prepared in 1% DMSO-PBS and incubated with SYPRO orange. No changes in SYPRO orange fluorescence was detected suggesting there is no aggregation or micellar formation. 0.1% Triton-X100 and 5 μg RBD as positive controls for micelles and hydrophobic sites, respectively (n=3, mean ±SEM; one-way ANOVA with Dunnet's test for multiple comparisons; values compared to 25 μM Bifonazole).

A)

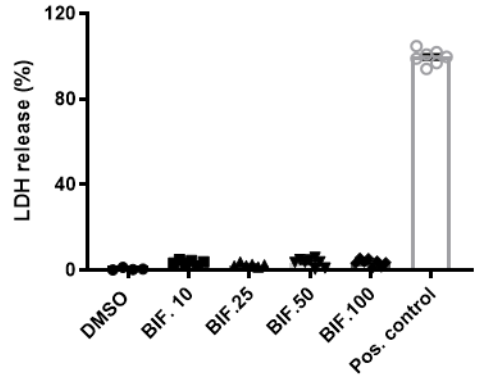
LDH release (%)
120
80
40
0
DMSO
BIF.10
BIF.25
BIF.50
BIF.100
Pos. control

B)

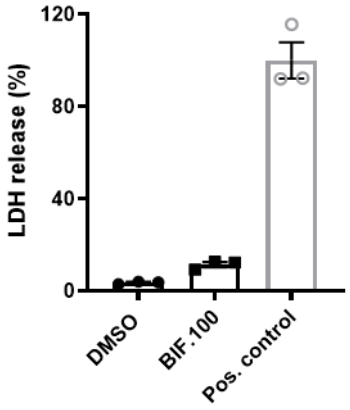
LDH release (%)
120
80
40
0
DMSO
BIF.100
Pos. control

C)

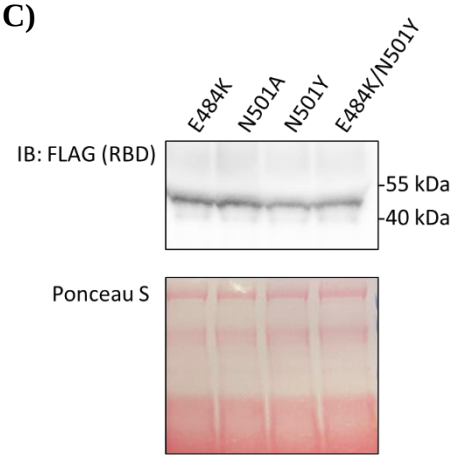
E484K
N501A
N501Y
E484K/N501Y
IB: FLAG (RBD)
55 kDa
40 kDa
Ponceau S

D)

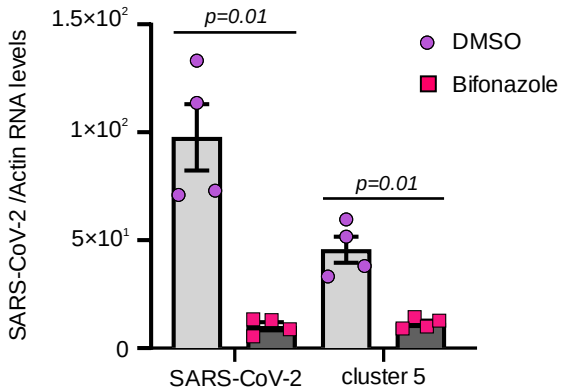
SARS-CoV-2 /Actin RNA levels
1.5×10²
1×10²
5×10¹
0
p=0.01
p=0.01
DMSO
Bifonazole
SARS-CoV-2
cluster 5

E)

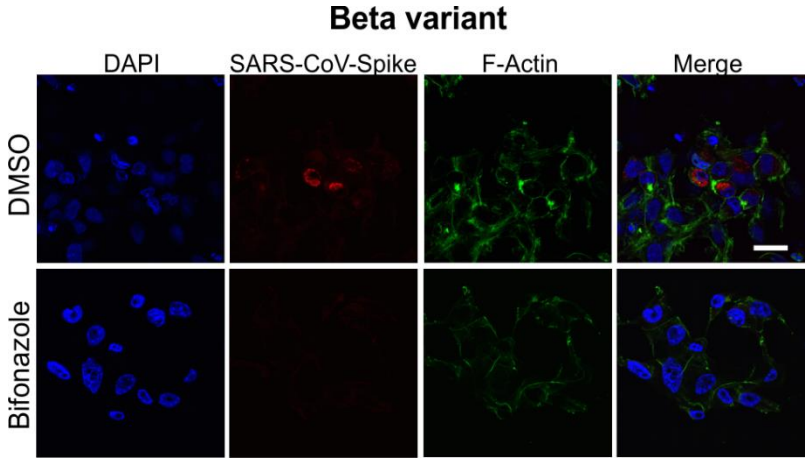
Beta variant
DAPI
SARS-CoV-Spike
F-Actin
Merge
DMSO
Bifonazole

F)

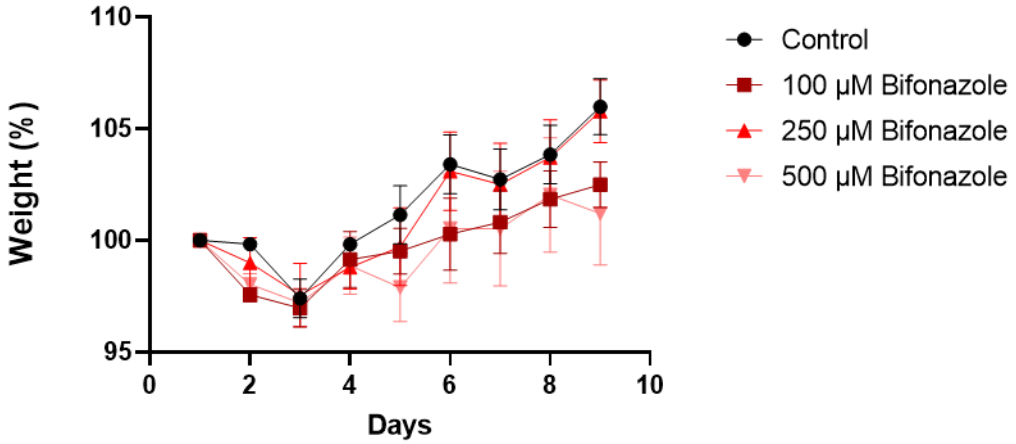

G)

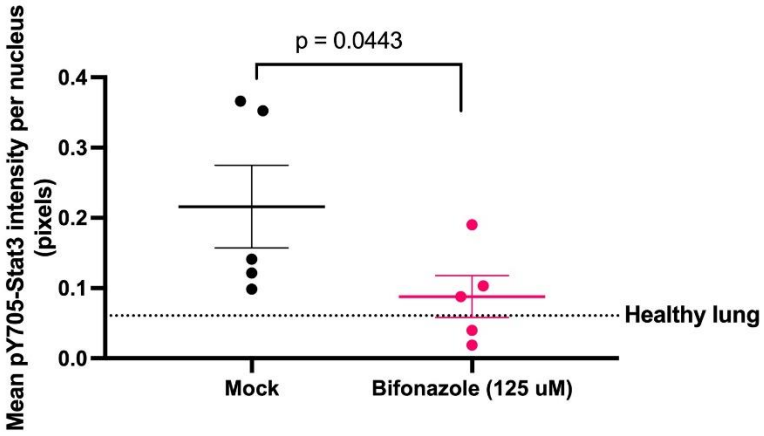

Supplementary Figure 6. Impact of Bifonazole on SARS-CoV-2. A-B) Bifonazole does not impact cell viability. Bifonazole cytotoxicity was assessed over a 48-hour time period time using an LDH assay and increasing dosage of the drug in Vero hTMPRSS2 (A) or A549-hACE2 (B). Data are the means +/- SEM from two experiments performed in triplicate (A) or one experiment performed in triplicate (B). **C)** 15 µl of RBD mutant supernatants used in Figure 5H were subject to western blotting for FLAG (top) and Ponceau stained for total protein detection (bottom).
D) Bifonazole inhibits SARS-CoV-2 cluster 5 infection. Vero hTMPRSS2 were pre-treated with Bifonazole (100 µM) for 15 minutes before infection with the original SARS-CoV-2 or the variant of concern (cluster5) at MOI 0.1. Viral RNA levels were determined 48h post infection by qPCR

(*n* = 4, mean ± SEM with student's t-test). **E)** Vero hTMPRSS2 cells were seeded on glass cover slips before a 15-minute treatment with Bifonazole (100 μM) and subsequent infection with SARS-CoV-2 Beta variant (MOI 0.1). SARS-CoV-2 spike protein was visualized using immunostaining and confocal imaging. Nuclei were stained using DAPI and F-Actin using Phalloidin ((bar = 20 μm). **F)** Dose escalation of Bifonazole in Balb/c mice. Balb/c mice (5 per group) were anaesthetized daily and treated intranasally with 0, 125 μM, 250 μM, or 500 μM Bifonazole in 10 μl containing 3.25% DMSO for 9 days. Weights were recorded daily and mice were assessed for wellness according to the ethical standards of the Canadian Council on Animal Care and with the Animals for Research Act. **G)** Lungs were harvested from K18-hACE2 mice and processed for IHC staining for pY705-Stat3. All stained sections were scanned using the AxioScan.Z1 and quantified for DAB intensity.